Performance of Large-Size Superconducting Coil in 0.21T MRI System

K. H. Lee*, M. C. Cheng, K. C. Chan, *Member, IEEE*, K. K. Wong, Simon S. M. Yeung, *Member, IEEE*, K. C. Lee, Q. Y. Ma, *Member, IEEE*, and Edward S. Yang, *Fellow, IEEE*

***Abstract*—A high-temperature superconductor (HTS) was used on magnetic resonance imaging (MRI) receiver coils to improve image quality because of its intrinsic low electrical resistivity [1], [2]. Typical HTS coils are surface coils made of HTS thin-film wafers. Their applications are severely limited by the field of view (FOV) of the surface coil configuration, and the improvement in image quality by HTS coil is also reduced as the ratio of sample noise to coil noise increases. Therefore, previous HTS coils are usually used to image small *in vitro* samples, small animals, or peripheral human anatomies [3]–[5]. We used large-size HTS coils (2.5-, 3.5-, and 5.5-in mean diameter) to enhance the FOV and we evaluated their performance through phantom and human MR images. Comparisons were made among HTS surface coils, copper surface coils, and cool copper surface coils in terms of the signal-to-noise ratio (SNR) and sensitivity profile of the images. A theoretical model prediction was also used to compare against the experimental result. We then selected several human body parts, including the wrist, feet, and head, to illustrate the advantage of HTS coil over copper coil when used in human imaging. The results show an SNR gain of 200% for 5.5-in HTS coil versus same size copper coils, while for 2.5- and 3.5-in coils it is 250%. We also address the various factors that affect the performance of large size HTS coils, including the coil-to-sample spacing due to cryogenic probe and the coil-loading effect.**

***Index Terms*—High-temperature superconducting (HTS), magnetic resonance imaging (MRI), surface receiver coil.**

I. Introduction

HIGH-TEMPERATURE superconductors (HTS) have been studied for over a decade for application as magnetic resonance imaging (MRI) receiver coils [6], [7]. Since the noise of an MRI receiver coil is contributed by two major sources, the sample noise arising from the coupling of the lossy sample and the coil noise from the resistance of the coil itself, reducing either one of them will enhance the quality of the image. The signal-to-noise ratio (SNR) of the images obtained by the coil is inversely proportional to the square root of sample resistance and coil resistance [6]

$$\mathrm{SNR} \propto \frac{B_1}{\sqrt{R_c T_c + R_s T_s}} \tag{1}$$

where B_1 denotes the B field generated by passing a unit current around the coil, R_c denotes the coil resistance, R_s denotes the sample resistance, T_c denotes the coil temperature, and T_s denotes the sample temperature.

HTS is a superconductor that has relatively high critical temperature. Typical HTS material such as Yttrium Barium Copper Oxide (YBCO) has a critical temperature higher than the boiling point of liquid nitrogen (YBCO: 90 K). Because of the low resistivity of the HTS material in the superconducting state, the coil noise can be substantially reduced if HTS material is used to fabricate the MRI receiver coil. The SNR of the image obtained can therefore be improved significantly using HTS coil if the coil noise dominates the total noise content. Since the sample noise is dependent on the frequency, and in turn the field strength of the system, the sample noise is usually substantially less than the coil noise in low-field systems (<1T) [8]. Another method to reduce sample noise is to use small coils, but this in turn reduces the field of view (FOV) [8]. Therefore, HTS coils are most beneficial in low-field systems or in imaging small samples. Previous results on HTS coils are mainly of imaging *in vitro* samples, small animals in high-field systems (>4T), or peripheral human anatomies in low-field systems [3]–[5].

HTS coils are usually made of thin-film HTS wafers and thus they are usually restricted to surface coil configurations. Surface coils excel with their good SNR on the surface of the imaging area. However, the signal intensity drops off as a function of distance from the surface of the coil. In this respect, HTS coils are always limited to image superficial areas.

Given the limitation of using an HTS thin-film wafer in a surface coil, the next technical challenge is to optimize the coil-to-sample spacing with sufficient thermal insulation. The use of cryogens to cool the HTS coil has posed a tough requirement on the thermal insulation between the cryogens and the imaged sample. Typical thermal insulation methods for HTS coil cryostat are Styrofoam packing and vacuum insulation. In either case, the separation between the coil and the sample is increased. This will decrease the sensitivity of the coil.

In short, the constraints of HTS coil have posed a limitation on its usage on humans. Here, we have used larger size HTS coils (2.5-, 3.5-, and 5.5-in diameter) to enhance the FOV and thus expand the application of the HTS coil to image deeper human anatomies. We have evaluated the advantage of the large-size HTS coil in human clinical applications in terms of the SNR gain in a 0.21T MRI system. We have also used a theoretical model to predict the SNR gain of the HTS coils over r.t. copper coil and cooled (by liquid nitrogen) copper coils of different sizes. The model gives a prediction on the results of phantom and human imaging in the 0.21T MRI system. It can also serve as a means to describe and evaluate the various factors that can improve the image quality by using the HTS coil.

Manuscript received May 4, 2003; revised February 14, 2004. *Asterisk indicates corresponding author.*

*K. H. Lee is with the Jockey Club MRI Engineering Center, the University of Hong Kong, Hong Kong, China (e-mail: leekarhof@hotmail.com).

M. C. Cheng, K. C. Chan, K. K. Wong, S. S. M. Yeung, K. C. Lee, Q. Y. Ma, and E. S. Yang are with the Jockey Club MRI Engineering Center, the University of Hong Kong, Hong Kong, China.

Digital Object Identifier 10.1109/TBME.2004.831539

II. Theoretical Model

In this theoretical model, we aim at predicting the relative SNR profile of r.t. copper coils, cooled copper coils, and HTS coils. In total, we modeled nine coils: room temperature (r.t.) copper coils, cooled copper coils, and HTS coils, with three sizes of coils for each type (2.5-, 3.5-, and 5.5-in diameter). We modeled the difference in SNR due to the:

1) sensitivity profile difference between coils of difference sizes;
2) difference in sample noise content due to difference in coil sizes;
3) difference in coil noise content due to difference in coil sizes, materials, and temperature.

The sensitivity profile can be modeled by the use of the signal intensity profile of a circular surface coil along the central axis perpendicular to the coil surface, which was given by [9]

$$B_1 \propto \frac{1}{a\left(1+\frac{x^2}{a^2}\right)^{3/2}} \tag{2}$$

where B_1 is the B field generated by passing a unit current around the coil and is proportional to the signal intensity of the detected signal. x denotes the distance from center of the coil, and a denotes the radius of the coil. The profile depicts a decreasing sensitivity as the distance from the coil surface increases.

The other two factors can be estimated by measurement of quality factors (Q-factors) of the coils. The Q-factors of an MRI receiver coil are expressed as

$$Q_{\text{unloaded}} = \frac{\varpi L}{R_{\text{coil}}} \tag{3}$$

$$Q_{\text{loaded}} = \frac{\varpi L}{R_{\text{sample}} + R_{\text{coil}}} \tag{4}$$

where ω is the resonant frequency of the coil in radian, L is the inductance, R_{sample} is the sample resistance, and R_{coil} is the coil resistance. Here, we assumed that the inductance coupled from the sample is negligible. If we know the frequency and the inductance of the coil, the R_{coil} and R_{sample} can easily be calculated from

$$R_{\text{coil}} = \frac{\varpi L}{Q_{\text{unloaded}}} \tag{5}$$

$$R_{\text{sample}} = \frac{\varpi L}{Q_{\text{loaded}}} - \frac{\varpi L}{Q_{\text{unloaded}}}. \tag{6}$$

For the copper coils, the inductance of the coil can be deduced from the capacitance value of the coil and the frequency

$$f = \frac{1}{2\pi\sqrt{LC}}. \tag{7}$$

The Q-factor of the coils can be obtained by experimental measurements. In our study, these values were taken at the isocenter of a home-built 0.21T MRI system. The loading is a $13 \times 17.5 \times 17.5$ cm rectangular phantom filled with 3.3-g/liter $CuSO_4$ solution (electrical conductivity $\sim$1000 μS/cm, dielectric constant $\sim$80). The coil is placed in close proximity to the phantom to represent the loaded condition. In case of cooled copper coils and HTS coils, the coils have to be placed inside a cryostat filled with liquid nitrogen, with the coil-to-sample distance is 2.1 cm. Both the Q-factors under the loaded and unloaded conditions of all coils were measured. The coils were inductively coupled to the pick-up loop, and the Q-factors were measured by an Agilent 8753ES Network Analyzer. Measurements of the r.t. copper coils and cooled copper coils are given in Table I.

TABLE I
Q-Factor Measurements of Copper Coils

Coil type	Size (in.)	Q-factor (Unloaded)	Q-factor (Loaded)	C (pF)	L (uH)	R_{coil} (mΩ)	R_{sample} (mΩ)
r.t. Cu coils	2.5	123	122	3290	0.099	44.5	0.3
	3.5	123	113	1980	0.165	74.2	6.5
	5.5	123	105	1133	0.2887	130	22
Cooled Cu coils	2.5	271	269	3290	0.099	20.2	0.1
	3.5	273	245	1980	0.165	33.4	3.8
	5.5	207	149	1133	0.2887	77.1	30

TABLE II
Comparison of Q-Factors of HTS Coil Inside and Outside Magnet

	Coil outside magnet (unloaded)	Coil in magnet isocenter (unloaded)
2.5" HTS coil	6000	1450
3.5" HTS coil	10000	1100
5.5" HTS coil	14000	1320

The coils we used in the cooled and r.t. cases are the same. The frequency change after we cooled the coils is less than 2%, so we assume that the inductance remained unchanged after the coil is cooled. Here, we can see that the coil resistance is halved after cryogenic cooling.

The HTS coils that we used are made from thin-film YBCO wafers. The wafers are patterned by photolithography into an interdigitated pattern [6]. The pattern provides a resonant frequency, and the capacitance given by the interdigitated fingers is [10]

$$C(pf) = \frac{\varepsilon_{\text{re}} 10^{-3} K(k)(n-1)l}{18\pi K'(k)} \tag{8}$$

where ε_{re} is the relative effective dielectric constant. $K(k)$ and $K'(k)$ are the elliptic integral of the first kind and its complement. n is the number of interdigitated fingers, and l is the length of the fingers. In our study, the substrate of the film is made of sapphire, with an ε_{re} value of 11.7. Because the YBCO is deposited on one side of the substrate only, the effective dielectric constant is the average ε_{re} of air and sapphire, which is 6.35.

Therefore, by using (7) and (8), we can deduce the resistance of the coil by the Q-factor measurements and the dimensions of the interdigitated pattern.

Here, we can see that the ac resistance of HTS coil in the superconducting state is still in the milli-ohm range because of the skin-depth effect (see Table III). A substantial drop of the Q-factors in the magnet isocenter is due to rapid influx of quantized magnetic flux vortices as the lower critical field of the HTS material was exceeded [7] Table II.

By holding all other factors constant, the relative SNR can be calculated from the sensitivity $\mathrm{B_1}$ and the noise content $(\mathrm{R_c} + \mathrm{R_s})$ according to (1). We plot the normalized SNR of the different coils in Figs. 1–3.

TABLE III
Q-FACTOR MEASUREMENTS OF THE HTS COILS

Coil size	Q-factor (unloaded)	Q-factor (loaded)	C (pF)	L (uH)	R_{coil} (mΩ)	R_{sample} (mΩ)
2.5”	1450	1300	3003	0.109	4.157	0.48
3.5”	1100	900	1695	0.193	9.7	2.16
5.5”	1320	890	1190	0.275	11.52	5.56

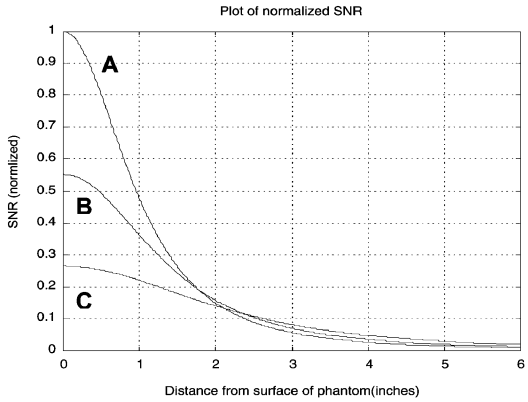

Fig. 1. SNR profile of circular r.t. copper surface coils of different sizes [A(2.5-in coil), B(3.5-in coil), C(5.5-in coil)].

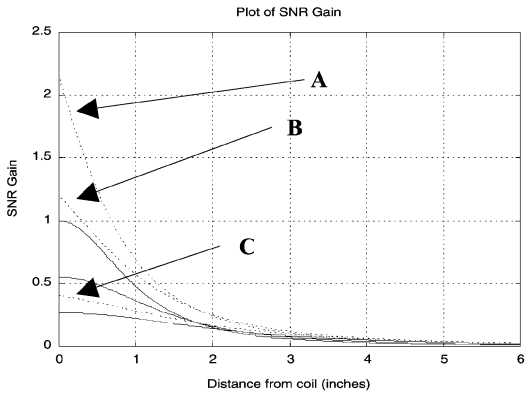

Fig. 2. SNR profile of the cooled copper coil (dotted line) as compared to copper coil (solid line). A is 2.5-in cooled copper coil. B is 3.5-in cooled copper coil. C is 5.5-in cooled copper coil.

The assumption that we have made here is that the pre-amp noise is negligible compared to coils noise and sample noise, and the variable factors are only the coil resistance, sample resistance, and profile difference between the different coil sizes.

The results showed that the cooled copper coils give a 210% SNR gain as compared to r.t. copper coils. The use of HTS coils provides a further 90% improvement in SNR as compared to cooled copper coils. The use of 5.5-in HTS coils provides an SNR gain of 300% as compared to r.t. copper coils. Furthermore, we can see that the choice between different sizes of HTS coils depends on how deep you want to image. As illustrated in our normalized SNR plot, we can see that the 5.5-in coils is preferred if we want to image anatomies deeper than 2-in from the coil.

We proceed to verify the result of this modeling by phantom and human images.

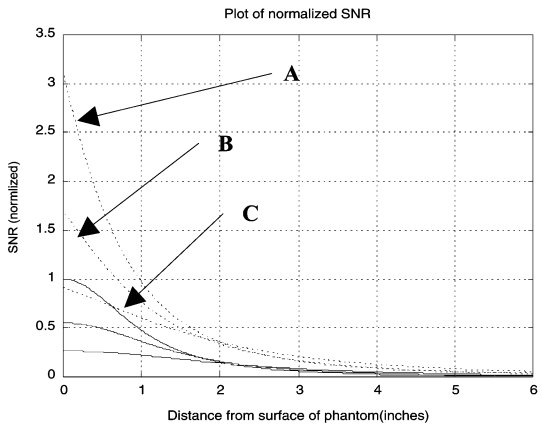

Fig. 3. Profile of the HTS coil (dotted line) as compared to copper coil (solid line). A is 2.5-in HTS coil. B is 3.5-in HTS coil. C is 5.5-in HTS coil.

III. MATERIALS AND METHOD

In order to verify the theoretical estimation, we imaged copper, cooled copper, and HTS surface coils in a home-built 0.21T MRI system. The magnet and gradient coils are made in the Electrical Engineering Institute of Chinese Academy of Science, the gradient control and power amplifier from Copley Control Corporation (Canton, MA), the console from Tecmag, Inc. (Houston, TX), and an in-house designed and built user interface. The gradient strength is 20 mT/m, the power of the RF amplifier is 300 W, and the computer console is run on a Pentium-IV 2.4 GHz PC. The copper surface coils, with mean diameters 2.5-, 3.5- and 5.5-in, respectively, were made from 3-M copper tapes and high-Q capacitors. The same coils were immersed into liquid nitrogen (LN) for the case of cool copper coils.

The HTS coils were made with thin-film YBCO ($T_c > 87$ K) wafers on sapphire substrates. They were fabricated into an interdigitated pattern by photolithography [6]. The patterned coil carries a resonant frequency of 8.8 ± 0.1 MHz. The HTS coils of different sizes are shown in Fig. 4.

Both the HTS coils and the cooled copper coils were cooled by LN. They were housed in home-made cryostats (shown in Fig. 5). The cryostats were basically made of fiber reinforced plastics (FRP) and styrofoam for thermal insulation. The cryostats also contain the tuning plate for fine frequency tuning and the pickup loop for signal pickup and matching.

Images of the rectangular phantom ($13 \times 17.5 \times 17.5$ cm rectangular phantom filled with 3.3 g/l Cu_2SO_4 solution) were taken with the same imaging parameters (2DSE, TR/TE: 400/31 ms, matrix size: 256×256. NEX: 2, FOV: 180×180 mm). The settings were the same for all cases, except that the cooled copper coils and HTS coils were placed inside the cryostat, and the copper coil was placed immediately beside the phantom to maximize the filling factor.

IV. EXPERIMENTAL RESULTS

A. Phantom Imaging Results

The images of the copper coil as well as the cool copper coil are given in Table IV.

The signal intensity profiles of the images along the coil central axis were taken. The profiles were smoothed within a

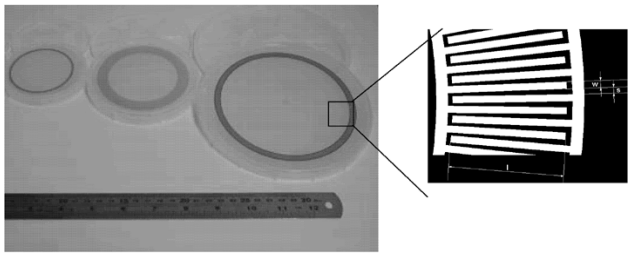

Fig. 4. HTS coils made of 3-, 4-, and 6-in wafers (from left to right). Mean diameters of the coil pattern are 2.5, 3.5, and 5.5, respectively. Interdigitated pattern is shown on the right side.

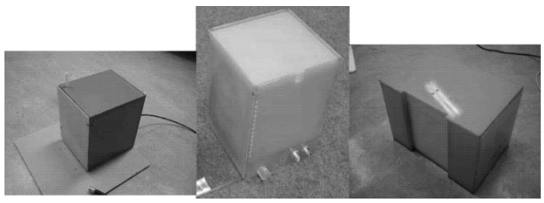

Fig. 5. Different types of cryostats for 2.5-, 3.5-, and 5.5-in coils (from left to right).

TABLE IV
IMAGES OF THE PHANTOM

	2.5”	3.5”	5.5”
Copper coil	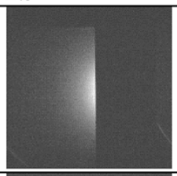	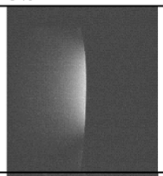	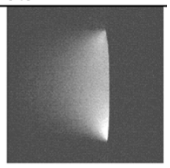
Cooled Copper coil	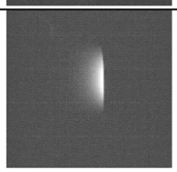	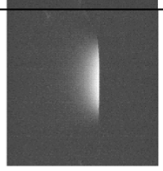	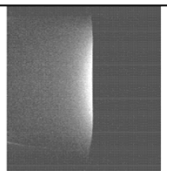
HTS coil	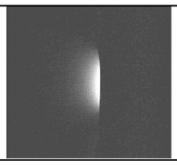	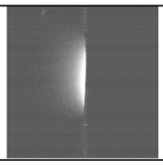	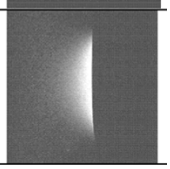

window of four pixels. The noise content in each of the images was taken as the standard deviation (SD) of the signal intensity in areas outside the phantom.

$$\mathrm{SNR} = \frac{\mathrm{Mean}_{\mathrm{signal}} - \mathrm{Mean}_{\mathrm{noise}}}{\mathrm{SD}._{\mathrm{noise}}}. \tag{9}$$

The plots of the SNR along the central axis of the surface coil, as calculated by (9), are given in Table V.

The SNR gain near the coil surface is summarized in Tables VI and VII.

We can see that the gain of HTS coils over copper coil is 200%–250%, and 130%–180% over Cooled copper coils. The discrepancy between the experimental result and the theoretical calculations can be attributed to the following factors.

1) The effect of Q value on the bandwidth of the coil. The imaging bandwidth was taken to be 12 kHz. For an HTS coil of $\mathrm{Q-factor} = 1000$, at $\mathrm{f} = 8.919$ MHz, the bandwidth of the coil is only about 9 kHz. With the coil bandwidth less than the acquisition bandwidth, part of the signal may be attenuated. Also, tuning becomes very critical, as a slight offset from the center frequency will lead to signal mismatch.
2) The theoretical calculation assumes that the noise contributed by the pre-amp and the cable length between the coil and the pre-amp is negligible compared with the sample noise and the coil noise. In the case of the HTS coil, where the coil noise is substantially reduced, the effect from the pre-amp and the cable will be more eminent and offset the SNR gain of the HTS coil.

TABLE V
SOLID LINE CORRESPONDS TO 2.5-in COILS, DOTTED LINE CORRESPONDS TO 3.5-in COIL, AND DASHED LINE CORRESPONDS TO 5.5-in COILS

	SNR plot
Copper coil	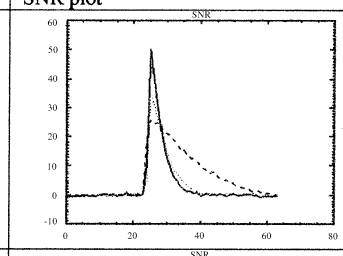
Cooled Copper coil	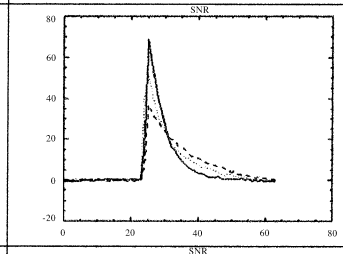
HTS coil	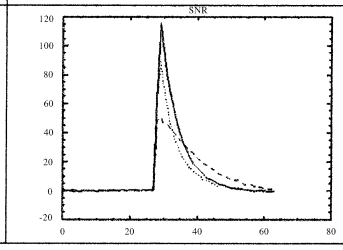

TABLE VI
SNR GAIN OF THE COOLED COPPER COIL VERSUS COPPER COIL IMAGES

	SNR (r.t. Copper coil)	SNR (Cooled Copper coil)	SNR Gain (Cooled Copper coil vs Copper coil)
2.5”	50	70	1.4
3.5”	35	50	1.429
5.5”	25	38	1.52

TABLE VII
SNR GAIN OF THE HTS COIL VERSUS COOLED COPPER COIL AND COPPER COIL IMAGES

	SNR (HTS coil)	SNR Gain (HTS coil vs r.t. Copper coil)	SNR Gain (HTS coil vs Cool Copper coil)
2.5”	118	2.36	1.69
3.5”	90	2.571	1.8
5.5”	50	2	1.32

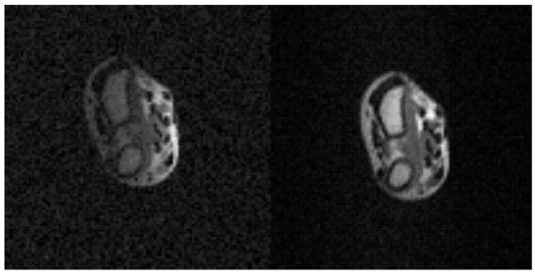

Fig. 6. Comparison axial image of the wrist [2.5-in copper coil (left) versus 2.5-in HTS coil (right)]. SNR gain 2.3 (at 0.5 in from cryostat surface).

3) During signal reception, the frequency gradient coil may induce current in the HTS coil. A slight heat up of the coil may offset the SNR gain.

Referring to the experimental data, the 2.5-in HTS coil offers a higher SNR at penetration within 1 in from the surface, while the 5.5 in is probably a better choice for deeper penetration.

With this result, we proceed to investigate the performance of HTS coil on human imaging.

B. Human Imaging Results

In order to verify the performance of HTS coil in human imaging, we imaged different human body parts by using copper coils and HTS coils. As obtained from the result of phantom images, we know that 2.5- or 3.5-in coils are better for imaging within 1 in from the coil surface, while 5.5-in coils should be used for deeper penetration. Therefore, we have tried wrist and foot imaging by 2.5- and 3.5-in coils and head imaging using 5.5-in coils in the 0.21T MRI system. All images are from normal healthy volunteers, with the same pulse sequences (2DSE, TR/TE: 400/31 ms, matrix size: 256×256, NEX: 2, FOV: 180×180 mm) in the 0.21T MRI system (see Figs. 6–8).

The results show that with the use of 2.5- and 3.5-in coils, the SNR gain is about 230%–250%. While for deeper anatomies, such as the brain cortex, the 5.5-in HTS coil is used instead, which provides about 200% SNR gain which provides about 200% SNR gain (see Fig. 9). These results agree with the phantom imaging results.

V. Conclusion and Discussion

This paper describes an attempt to use a large-size HTS coil for MR imaging and quantifies the performance of HTS coils of different sizes as compared to copper coils and cooled copper coils. The use of a large-size HTS coil is to cater for the requirement of enhanced FOV for human imaging, and the result justified the SNR advantage by using such coils. A model is also devised to predict the performance of HTS coils.

The phantom and human images agree well with each other. The SNR gain of 2.5- and 3.5-in HTS coils is about 230%–250% as compared to r.t. copper coils. The 5.5-in coil offers a lesser SNR gain ($\sim$200%), but it is more suitable for imaging deeper anatomies.

The theoretical could not accurately predict the gain in each case and provides a reasonable limit on the SNR offered by each coil. The model also provides ground to study the two effects

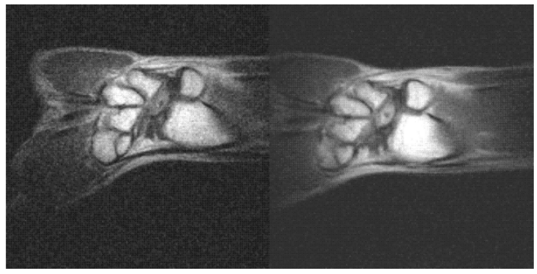

Fig. 7. Comparison saggital image of the wrist [2.5-in copper coil (left) versus 2.5-in HTS coil (right)]. SNR gain 2.62.

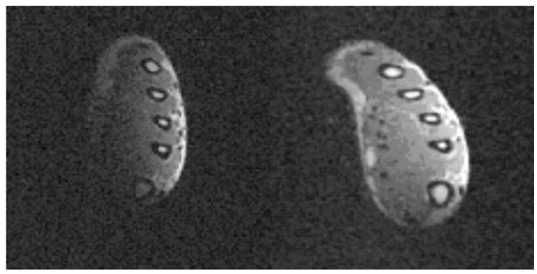

Fig. 8. Comparison axial image of the feet [3.5-in copper coil (left) versus 3.5-in HTS coil (right)]. SNR gain 2.26 (at 0.5 in from cryostat surface).

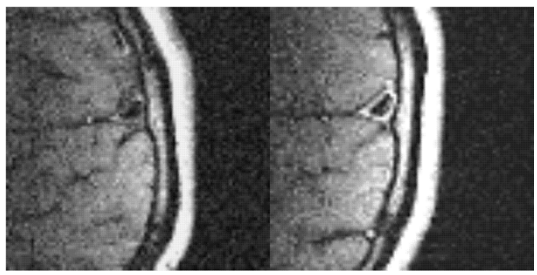

Fig. 9. Comparison coronal image of the brain (5.5- copper coil (left) versus 5.5-in HTS coil (right)]. Image is a close up at the occipital lobe of the brain. SNR gain 1.96 (at 1.2 in from the cryostat surface).

that may substantially affect the SNR gain: sample noise contribution and the effect by the sample-to-coil separation.

A. Sample Noise Contribution

As discussed previously, the SNR gain given by the HTS coils is most significant when the coil noise dominates the total noise [refer to (1)]. We can estimate the sample noise-to-coil-noise ratio by using

$$\frac{R_{\text{sample}}}{R_{\text{coil}}} = \frac{Q_{\text{unloaded}}}{Q_{\text{loaded}}} - 1. \tag{10}$$

Table VIII summarizes the sample noise proportion as compared to coil noise when the coil is loaded with the phantom.

As the HTS coil has a significantly reduced coil noise, the sample noise tends to become more significant as compared to coil noise. The sample noise-to-coil-noise ratio gets even bigger when the coil size is increased. As seen from the table, the sample noise from a phantom contributes sample noise which is 10%–20% of the coil noise in an 2.5- or 3.5-in HTS coil. The ratio increases drastically to about 50% when 5.5-in HTS coil is used. The increase in this ratio limits the SNR gain against copper coil.

TABLE VIII
SAMPLE NOISE-TO-COIL-NOISE RATIO

	Q-factor with the coil in magnet isocenter		
	Unloaded	Loaded with phantom	Sample noise: Coil noise Ratio
2.5" HTS	1450	1300	0.115
3.5" HTS	1100	900	0.222
5.5" HTS	1320	890	0.483
2.5" Cooled Copper	271	269	0.0074
3.5" Cooled Copper	273	245	0.114
5.5" Cooled Copper	207	149	0.389

TABLE IX
SAMPLE NOISE TO COIL NOISE RATIO FOR LOADED CONDITION BY HUMAN PARTS

	Q-factor with the coil in magnet isocenter			Sample noise: Coil noise Ratio	
	Unloaded	Loaded with human wrist	Loaded with human head	wrist loading	head loading
2.5" HTS	2327	1691	1297	0.376	0.794
3.5" HTS	1691	1230	1047	0.375	0.615
5.5" HTS	1320	968	538	0.364	1.455
2.5" Cooled Copper	271	246	231	0.102	0.173
3.5" Cooled Copper	273	250	227	0.092	0.203
5.5" Cooled Copper	207	183	156	0.131	0.327

In human imaging, the coil is loaded by the imaged body parts. Different parts of the body offer different levels of sample noise to the coil. Table IX summarizes the effect when loaded with the head and the wrist of a healthy normal volunteer.

As shown in the table, the loading of the wrist contributes sample noise which is about 35% of the coil noise for all sizes HTS coils. However, the loading of the head contributes sample noise which is about 70% of the coil noise for 2.5- and 3.5-in coils, and 140% for 5.5-in coils. The effect of the substantial amount of sample noise from the head on the 5.5-in coil can readily be reflected from the loaded Q of the 5.5-in HTS coil. Significant reduction in the Q-factor after sample loading limits the SNR gain.

B. Coil-to-Sample Spacing

The sample-to-coil separation is another major factor that diminishes the SNR gain of HTS coil. This separation arose from the use of cryostat in cryogenically cooled coils. As deduced from the theoretical prediction in this paper, increased sample-to-coil separation reduces the sensitivity of the coil to the signal from the sample. Assuming a coil-to-sample separation of 2.1 cm, which is measured from the cryostat that we use here, the reduction in sensitivity can be summarized in Table X.

TABLE X
REDUCTION OF SENSITIVITY OF HTS COIL DUE TO A COIL-TO-SAMPLE SPACING OF 2.1 cm

	Cooled Copper Vs Copper	HTS Vs Copper	HTS Vs Cooled Copper
2.5" coils	2.15	3.1	1.44
3.5" coils	2.18	3.1	1.42
5.5" coils	1.33	3	2.26

Sample-to-coil distance is unavoidable due to the thermal insulation requirement of HTS coils. In Table X, we can see that the effect is most serious for small coils, while for the 5.5-in coil, the drop in sensitivity is only about 15% with such sample-to-coil separation. With the use of better insulation methods, such as vacuum cryostats, the reduction in signal sensitivity can be minimized, and thus the SNR gain can be increased. However, vacuum cryostats are expensive and bulky. In the application of human imaging, the increase in SNR gain may be offset by these two factors, especially when large coils are used.

To summarize, the human wrist, feet, TMJ, eyeball, carotid artery, etc., are good application candidates for these coils. The use of larger HTS coils (5.5 in) also provides SNR gain ranging from 150%–200% as compared to copper surface coils and will be beneficial for the imaging of deeper areas such as the brain cortex or cardiac applications. The impact of this HTS surface coil will be most prominent in areas which combine the use of surface coil technology and low-field machines. Potential areas include interventional MRI and orthopedic imaging. Interventional MRI systems usually adopt open magnets to provide spaces for interventionist access, and open magnets are, in general, low-field magnets. This, in turn, results in a comparatively low-image quality which is a major drawback of interventional MRI. With the use of HTS coils, the image quality can be enhanced, without the need to substantially modify the system. Orthopedic systems also use low-field systems due to cost consideration. HTS coils are useful in this area since some orthopedic structures such as meniscus or thin cartilage may require a higher image quality and resolution. The application of HTS coil will expand even more when new coil configurations can be designed.

REFERENCES

[1] Q. Y. Ma, "RF applications of high-temperature superconductors," *IEEE Trans. Appl. Superconduct.*, vol. 9, pp. 3565–3568, June 1999.
[2] Q. Y. Ma *et al.*, "Superconducting RF coils for clinical MR imaging at low field," *Acad. Radiol.*, vol. 10, no. 9, pp. 163–169, Sept. 1999.
[3] S. E. Hurlston *et al.*, "A high-temperature superconducting Helmholtz probe for microscopy at 9.4T," *Magn. Reson. Med.*, vol. 41, pp. 1032–1038, 1999.
[4] J. Wosik *et al.*, "High-T_c superconducting *rf* receiver coils for magnetic resonance imaging of small animals," in *Proc. Applied Superconductivity Conf.*, VA, 2000, pp. 17–22.
[5] J. C. Ginefri *et al.*, "High-temperature superconducting surface coil for *in vivo* micro-imaging of the human skin," *Magn. Reson. Med.*, vol. 45, pp. 376–382, 2001.

[6] R. S. Withers *et al.*, "Thin-film HTS probe coils for magnetic resonance imaging," *IEEE Trans. Appl. Superconduct.*, vol. 3, pp. 2450–2453, 1993.
[7] R. D. Black *et al.*, "A high-temperature superconducting receiver for nuclear magnetic resonance microscopy," *Science*, vol. 259, no. 793, 1993.
[8] M. D. Harpen, "Sample noise with circular surface coils," *Med. Phys.*, vol. 14, no. 4, 1987.
[9] C. L. Partain, R. R. Price, J. A. Patton, M. W. Kulkarni, and A. E. James *et al.*, *Magnetic Resonance Imaging*, 2nd ed. Philadelphia, PA: Saunders, vol. II.
[10] K. C. Gupta, *Microstip Lines and Slotlines*, 2nd ed. Boston, MA: Artech House, 1996.

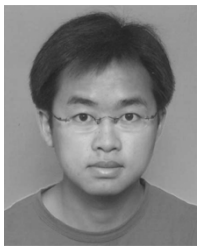

K. H. Lee received the B.S. degree in electrical and electronic engineering from the University of Hong Kong, Hong Kong, in 1999 and the M.S. degree in bioengineering from the University of Pennsylvania, Philadelphia, in 2000.

From August 2000 to July 2001, he worked for Medtronic, Inc, as a Regulatory/Quality Affairs Specialist in the Asia/Pacific Region. After this, he joined the Jockey Club Magnetic Resonance Imaging Engineering Center in the University of Hong Kong as a Research Engineer. He has participated in the development of HTS thin-film coils and is a coinventor of the HTS-tape volume coil. His research interests include radiofrequency coils for MRI systems and medical image and signal processing.

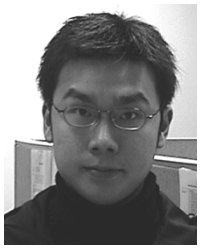

M. C. Cheng received the B.Sc. degree in physics in 2001 and the M.Phil. degree in electrical and electronic engineering in 2004, all from the University of Hong Kong, Hong Kong.

He demonstrated the first Bi-2223 HTS tape RF volume coil for MRI with human imaging and was published in the *Proceedings of International Society of Magnetic Resonance in Medicine* in 2003 and 2004. He holds one pending U.S. patent. His current research interests include HTS tape RF coils and cryogen design for clinical applications.

K. C. Chan (M'02) received the B.S. degree in engineering and M.S. degree in philosophy from the University of Hong Kong, Hong Kong, in 1997 and 2000, respectively.

His research interests include MRI RF coil design, MRI System integration, applications of HTS materials, and electromagnetic simulation. He has been one of the core members to set up the Jockey Club MRI Engineering Center and the attached research laboratory at the University of Hong Kong. He has participated in the development of the Open Mobile MRI vertical system. He incorporated the HTS technology into MRI by designing the HTS RF coil and the probe integration for both low-field and high-field MRI systems.

K. K. Wong received the B.Eng. and M.Phil. degrees from the University of Hong Kong, Hong Kong, in 1997 and 2000.

He is currently a Research Associate at the Jockey Club MRI Engineering Center, University of Hong Kong. His research interests include functional MRI, contrast-enhanced blood volume mapping, high-temperature superconducting coil imaging, as well as acupuncture point brain mapping.

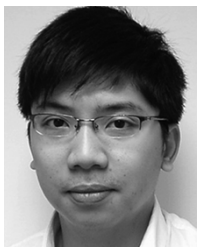

Simon S. M. Yeung (M'02) received the M.Phil. degree in electrical engineering from University of Hong Kong, Hong Kong.

He is a member of the Jockey Club MRI Engineering Center, University of Hong Kong. His research interests include HTS coil array signal processing.

Mr. Yeung is a member of ISMRM.

K. C. Lee is pursuing the B.S. degree in information engineering at the University of Hong Kong, Hong Kong.

He was a Trainee in the Jockey Club MRI Engineering Center in 2003.

Q. Y. Ma (M'99) received the Ph.D. degree from Columbia University, New York, NY, in 1990.

He spent the next three years at the University of British Columbia in Canada as a Research Associate. He joined the Department of Electrical Engineering, Columbia University, in 1994 and became an Associate Professor in 1997. Currently, he is an Associate Professor in the Department of Electrical and Electronic Engineering and the Deputy Director of the Jockey Club MRI Engineering Center, University of Hong Kong, as well as an Associate Professor of Radiology at Harvard Medical School. He has been conducting research in the area of microelectronic materials and devices, biomagnetic sensors, and medical instrumentation. His current research interests include superconducting electronics, biomedical sensors, RF coils, brain sensing and mapping, and MR imaging technologies. He holds seven patents and is the author or coauthor of over 160 journal and conference papers.

Dr. Ma is a member of AAAS, APS, EMBS, ISMRM, and MRS. He received the NSF Career Award and the Most Impressive Presentation Award of the 11th International Workshop on Future Electron Devices.

Edward S. Yang (S'60–M'61–SM'74–F'92) received the B.S., M.S., and Ph.D. degrees from Cheng-Kung Universitty (Taiwan), Oklahoma State University (Stillwater), and Yale University (New Haven, CT), respectively.

He joined the Electrical Engineering Department, Columbia University, New York, NY, in 1965 and was the Chairman from 1986 to 1989 and 1993 to 1996. He had a long association with IBM both as an Engineer and a Researcher from the early 1960s to mid 1990s. He was the Chair Professor of the Microelectronics Engineering Department, Electrical and Electronic Engineering, Hong Kong University (HKU), Hong Kong, from 1997 to 2003. Currently, he is the Director of The Jockey Club Magnetic Resonance Imaging Engineering Center, University of Hong Kong. He has been responsible for developing major engineering research and educational centers including the NSF Center for Telecommunication Research and the Microelectronics Science Laboratories at Columbia and the MRI Engineering Centre at HKU. He was a Consultant to Exxon, W. R. Grace, IBM Research, and RCA and has been an Advisor to SMIC and the governments of Shanghai and Beijing. He has published 180 papers and two books; the latter have been translated into Chinese, Italian, Japanese, and Korean. At present, he is involved in research projects in magnetic resonance imaging technology and applications to clinical medicine and microelectronics.